Near-Real-Time Estimation of Water Vapor Column From MSG-SEVIRI Thermal Infrared Bands: Implications for Land Surface Temperature Retrieval

Yves Julien, José A. Sobrino, Cristian Mattar, and Juan C. Jiménez-Muñoz

***Abstract*—The Meteosat Second Generation-Spinning Enhanced Visible and Infrared Imager (MSG-SEVIRI) instrument provides observations of half the globe every 15 min, at low spatial resolution. These data are an invaluable tool to observe daily to yearly cycle of land surface temperature (LST), as well as for various early warning systems. However, advanced algorithms for LST estimation requires a previous estimation of the water vapor (WV) column above the observed pixel, for which no instantaneous retrieval methods are yet available, and therefore hinders their implementation in a near-real-time processing chain for MSG-SEVIRI data. This work analyzes three different formulations for such WV retrieval, which are compared to independent WV estimates obtained from radiosoundings. The best suited algorithm is then selected for WV estimation and compared with the results obtained with a previous noninstantaneous algorithm [23]. This comparison shows that, in spite of retrieval errors higher than the ones reported in the literature, the estimated WV compares relatively well with *in situ* data, while allowing for an instantaneous estimation of WV column (every 15 min). Error propagation analysis and direct comparison show that the observed increase in WV estimation error has a negligible influence on LST retrieval. Therefore, this algorithm is well suited to be implemented in a near-real-time processing chain for MSG-SEVIRI data.**

***Index Terms*—Land surface temperature (LST), Meteosat Second Generation-Spinning Enhanced Visible and Infrared Imager (MSG-SEVIRI), water vapor (WV).**

I. Introduction

THE Meteosat Second Generation (MSG) satellite platform, with its geostationary orbit, provides valuable information to the scientific community. The Spinning Enhanced Visible and Infrared Imager (SEVIRI) instrument, onboard MSG, acquires data from visible to thermal infrared (TIR) wavelengths at coarse resolution (3 km at nadir) every 15 min. Therefore, numerous applications have been carried out, such as vegetation monitoring [7], [21], dead fuel moisture estimation [15], fire monitoring [2], [9], air temperature estimation [16], land surface temperature (LST) estimation [13], [22], [24], cloud detection [6] or rainfall estimation [10]. Many of these applications are specifically dedicated to or dependent on LST estimation, which can be retrieved through split-window (SW) methods [11], among others. LST estimation depends, in turn, on the estimation of surface emissivity in TIR bands [12], and retrieval of total amount of water vapor (WV) increases the accuracy of the approach [20].

Within the framework of the CEOS-SPAIN project, the Global Change Unit of the University of Valencia is providing (among other tasks) near-real-time estimates of LST from MSG-SEVIRI data, to be uploaded onto a server from which these data will be available to the general public. To that end, near-real-time estimation of LST is required, and since advanced algorithms for LST estimation require the previous estimation of total WV column (among other parameters; for more details, see [22]), a near-real-time estimation of WV has to be carried out. Existing algorithms [19], [23] allow the estimation of WV column, although both algorithms exploit brightness temperature differences between two acquisitions to retrieve WV amount. This brightness temperature difference is set to at least 5 K for Schroedter-Homscheidt *et al.* [19] algorithm, while Sobrino and Romaguera [23] algorithm requires it to be above 10 K. As a result, near-real-time implementation of these algorithms is not straightforward since, depending on the time lapse chosen between acquisitions, various brightness temperature differences can be retrieved (provided they are above each method threshold), leading to different estimates of WV, assumed to be constant over the chosen time lapse. Up to 2013, MSG-SEVIRI WV was estimated at the Global Change Unit of the University of Valencia as an average of all valid estimates of WV column obtained by the application of Sobrino and Romaguera [23] algorithm for all possible 6-h-long time differences within a given day. However, this approach prevents a near-real-time estimation of LST since a whole day of data needs to be processed to retrieve the mandatory WV. Moreover, this approach assumes constant WV amount during one day, which can lead to artificial discontinuities between consecutive days. Therefore, a straightforward algorithm would be beneficial for all MSG-SEVIRI receiving stations.

Manuscript received July 28, 2014; revised November 4, 2014; accepted December 18, 2014. This work was supported in part by the Spanish Ministerio de Ciencia y Tecnología under Project AYA2011-29334-C02-01 (CEOS-SPAIN) and in part by Chilean Projects U-INICIA VID 4/06212 and Fondecyt-Initial 11130359 (CONICYT).

Y. Julien, J. A. Sobrino, and J. C. Jiménez-Muñoz are with the Global Change Unit, Image Processing Laboratory, University of Valencia, 46980 Valencia Spain.

C. Mattar is with the Laboratory for Analysis of the Biosphere (LAB), University of Chile, Santiago, Chile.

Color versions of one or more of the figures in this paper are available online at http://ieeexplore.ieee.org.

Digital Object Identifier 10.1109/TGRS.2015.2393378

The WV estimation method presented hereafter is designed to retrieve WV instantaneously, without any ancillary data (i.e., all needed information are retrieved from SEVIRI data only). Since SEVIRI sensor does not include the adequate bands in the visible wavelengths to estimate WV, this estimation can only be carried out from the available TIR SEVIRI bands. The need for instantaneous WV estimates also prevents the use of methods based on the WV daily cycle.

II. Data

Three different data sets have been used in this study: 1) real-time MSG-SEVIRI data received at the Global Change Unit of the University of Valencia; 2) atmospheric profile data sets for simulation purposes; and 3) radiosoundings launched at different permanent stations extracted from the University of Wyoming data set and used for validation purposes. These three data sets are described briefly hereafter.

A. MSG-SEVIRI Data

The MSG-SEVIRI data used in this study have been acquired using a direct-broadcast High Resolution Picture Transmission (HRPT) system implemented at the Global Change Unit of the University of Valencia since mid-2007. This system consists of a parabolic dish, a PC with the hardware and software to decode L-band data, and a set of storage devices to save all the received SEVIRI data. Since SEVIRI temporal resolution is 15 min, the received data amount to 96 images per day for each channel. Therefore, the storage space needed is 1 TB of data per month. In this paper, seven SEVIRI TIR bands located in the 6–14-μm spectral region have been used to retrieve WV, denoted as WV6.2, WV7.3, IR8.7, IR9.7, IR10.8, IR12.0, and IR13.4, where the number indicates the band central wavelength in micrometers. Fig. 1 shows the spectral response and location of SEVIRI TIR bands in comparison to a standard atmospheric transmissivity spectrum. Bands WV6.2 and WV7.3 are clearly located in a WV absorption region, whereas band IR9.7 is located in the ozone absorption region. Bands IR8.7, IR10.8, and IR12.0 are located in the so-called atmospheric windows (regions with high atmospheric transmissivity), and in particular, bands IR10.8 and IR12.0 are located in the SW region. As for band IR13.4, it is located in a CO_2 absorption. Only data from year 2010 were used in this work, and validation was carried out with SEVIRI data from the first week of January, April, July, and October, in 2010, in order to cover the annual variation of WV amplitude.

B. Atmospheric Profile Data Set

The atmospheric profiles used in the simulation procedure carried out in the framework of this study were extracted from the Thermodynamic Initial Guess Retrieval (TIGR) database [1]. In particular, a selection of 61 atmospheres from the TIGR database was performed, as proposed in Sobrino *et al.* [20]. This data set, referred hereafter as TIGR-61, includes global atmospheric conditions with 28 atmospheres assigned to the tropical model, 12 to the midlatitude summer model, 12 to the subarctic winter model, and 9 to the U.S. standard model). The mean WV value for all the atmospheric profiles included in TIGR-61 is (2.9 ± 1.7) g $\cdot$ cm^{-2}, with minimum and maximum values of 0.2 and 6 g $\cdot$ cm^{-2}, respectively.

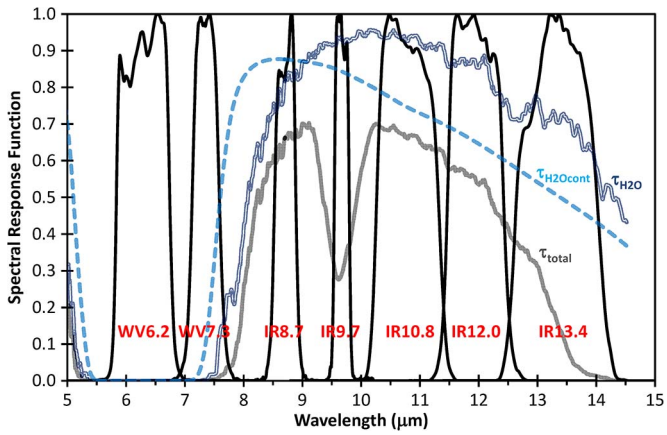

Fig. 1. SEVIRI TIR spectral response functions (black continuous line) overlapped to an atmospheric transmissivity spectrum for a standard atmosphere (gross gray line). The transmissivity spectrum only for the WV (H_2O) component (white with gray border line) and the WV column spectrum (dashed gray line) are also plotted.

C. Radiosonde Database

The radiosonde database used in this work consists of several atmospheric profiles freely available for download at Wyoming University server (http://weather.uwyo.edu/upperair/sounding.html). These vertical profiles were retrieved from different radiosonde types and models launched in several atmospheric conditions, such as temperate, tropical, desert, and subtropical, in order to span the whole amplitude of WV to be used in the LST algorithm retrievals. This database has been used in previous works for remote sensing applications and precipitable water long-term analysis [14], [18].

We selected all radiosonde stations located in South America, Europe, Africa, and Middle East, in order to cover the highest possible proportion of MSG-SEVIRI disk. The data acquired at these stations for year 2010 (first week of January, April, July, and October as for SEVIRI data) were used to retrieve alternative total WV column for validation purposes, as well as to build a rudimentary cloud mask associated to the WV estimates. Validation was carried out by comparing available radiosonde data to the closest (in space and time) SEVIRI estimation. This implies that we assume constant WV over SEVIRI pixel size for a 15-min duration.

III. Methods

A. Simulated Data

WV algorithms were developed from analysis of a complete simulated data set constructed under different surface and atmospheric conditions. At-sensor brightness temperatures for the SEVIRI TIR bands were reproduced from forward simulations based on the radiative transfer code MODTRAN-4 [5]. The surface was characterized from surface emissivities of 108 natural samples (soils, rocks, vegetation, water, snow/ice) extracted from the Advanced Spaceborne Thermal Emission and Reflection Radiometer (ASTER) spectral library [4]. The atmospheric conditions were characterized from the atmospheric profiles included in the TIGR-61 data set described earlier.

B. WV Algorithms and Coefficients

In order to estimate instantaneously the total amount of WV from MSG-SEVIRI data, different mathematical structures for the combination of the SEVIRI TIR bands were considered. After a preliminary analysis of results obtained with these combinations using the simulated data, a final selection of three algorithms was performed as follows:

$$\mathrm{WV1} = \mathrm{a}_0 + \mathrm{a}_1 \cdot \mathrm{WV062} + \mathrm{a}_2 \cdot \mathrm{WV073} + \mathrm{a}_3 \cdot \mathrm{IR087} + \mathrm{a}_4 \cdot \mathrm{IR097} + \mathrm{a}_5 \cdot \mathrm{IR108} + \mathrm{a}_6 \cdot \mathrm{IR120} + \mathrm{a}_7 \cdot \mathrm{IR134} \quad (1)$$

$$\mathrm{WV2} = \mathrm{a}_0 + \mathrm{a}_1 \cdot \mathrm{WV062} \cdot (\mathrm{IR108} - \mathrm{IR120}) \quad (2)$$

$$\mathrm{WV3} = \mathrm{a}_0 + \mathrm{a}_1 \cdot (\mathrm{IR108} - \mathrm{IR120}). \quad (3)$$

WV algorithms presented in (1)–(3) only use at-sensor brightness temperatures as input data. The WV algorithm given by (1) is a linear combination of all SEVIRI TIR bands. In this way, we take advantage of all the TIR spectral information, including also water absorption bands (WV062 and WV073). However, WV1 algorithm is expected to be more sensitive to accuracy of TIR measurements [e.g., Noise Equivalent Differential Temperature (NEΔT)], since the algorithm uses absolute values of at-sensor brightness temperatures. On the contrary, the algorithm given by (3) uses information extracted from only two TIR bands in the spectral region of 10–12 μm (known as the SW technique). Since this algorithm does not use absolute values of brightness temperatures but the difference between two bands, it is expected to be less sensitive to errors in TIR measurements. The algorithm given by (2) is based on the SW algorithm (3) but also includes information from one WV absorption band (WV062).

Table I presents the coefficients and estimation errors for (1)–(3) using the simulated data set. Coefficients were obtained from linear least squares minimization, whereas the total error (e_{WV}) were obtained from total sum of squares of the different errors according to the classical rules for error propagation, i.e.,

$$e_{\mathrm{WV}} = \sqrt{\sigma^2 + \sum_{i=1}^{N} \left[\left(\frac{\partial W}{\partial T_i} \right) e(T_i) \right]^2} \quad (4)$$

where σ is the standard error of estimation, T_i are the at-sensor brightness temperatures for the different SEVIRI bands $(i = 1, N)$, and $e(T_i)$ is the NEΔT, assumed to be 0.2, 0.1, 0.1, 0.3, 0.1, 0.15, and 0.4 K for SEVIRI bands WV6.2, WV7.3, IR8.7, IR9.7, IR10.8, IR12.0, and IR13.4, respectively (corresponding to the European Organization for the Exploitation of Meteorological Satellites' (EUMETSAT) technical specifications).

Results show that WV1 has the highest correlation coefficient (R^2) and the lowest error (0.6 g $\cdot$ cm^{-2}), whereas WV2 and WV3 provide similar results, with R^2 values of 0.78 and errors of 0.9 g $\cdot$ cm^{-2} in both cases.

C. Estimation of Radiosonde WV

WV estimates were derived from cloud-free atmospheric soundings following the method described by Ross and Elliot (2001). To this end, for each atmospheric profile, a simple cloud filter was implemented. This filter is based on high content of relative humidity (RH) to reveal cloud presence [25]. For this work, we discarded radiosonde, which contains any atmospheric level with RH values equal to or higher than 80%. Then, the saturated vapor pressure (e_s) was estimated by using

$$e_s = 611 \cdot 10^{(17.27T/(237.7+T))} \quad (5)$$

where T is the air temperature (in degrees celsius). This parameter is used to estimate the specific humidity

$$q_v = 0.622 \frac{e_s \cdot RH}{100 \cdot p} \quad (6)$$

where q_v is the specific humidity, e_{s} is the saturated vapor pressure estimated in (5), p and RH are atmospheric pressure and RH provided for each atmospheric pressure level, respectively. Once q_v is estimated, WV values were retrieved by integration of the whole atmospheric vertical profile, as follows:

$$\mathrm{WV} = 0.01 \int_{pz}^{p0} a_v dp \approx 0.01 \sum q_v \Delta p \quad (7)$$

where Δp corresponds to a finite difference for atmospheric pressure, 0 and z are the limits for integration along the whole atmospheric profile from 1000 hPa to the last atmospheric pressure level captured by the radiosonde (around 10 hPa or lower).

TABLE I
WV COEFFICIENTS FOR THE ALGORITHM GIVEN BY (1)–(3). COEFFICIENT OF DETERMINATION (R^2), STANDARD ERROR OF ESTIMATION (σ), AND TOTAL ERROR e_{WV} OBTAINED IN THE SENSITIVITY ANALYSIS ARE ALSO GIVEN

Coef	WV1	WV2	WV3
a_0	-70.7±1.0	1.400±0.014	1.403±0.014
a_1	-0.011±0.004	0.00692±0.00004	1.657±0.011
a_2	0.033±0.006		
a_3	-0.134±0.005		
a_4	0.083±0.002		
a_5	1.273±0.018		
a_6	-1.66±0.02		
a_7	0.725±0.015		
R^2	0.93	0.78	0.78
σ (g/cm^2)	0.5	0.8	0.8
e_{WV} (g/cm^2)	0.6	0.9	0.9

IV. RESULTS AND DISCUSSION

We estimated WV from MSG-SEVIRI data by using all three algorithms (1)–(3) and over all selected radiosonde stations, which we compared to clear-sky (see Section III) radiosonde WV estimates, considered as ground truth for this study. When considering all stations, the RMSE obtained for each algorithm are 3.24 g $\cdot$ cm^{-2} for WV1, 1.12 g $\cdot$ cm^{-2} for WV2, and 1.25 g $\cdot$ cm^{-2} for WV3. These errors are quite high when compared to other existing algorithms (6.8 mm, 0.68 g $\cdot$ cm^{-2}, for [19]; 0.5 g $\cdot$ cm^{-2} for [23]), particularly for WV1. We also carried out simulations including an observation angle dependence of (1)–(3), although the improvement in retrieved RMSE was not substantial (not shown). When looking at the spatial distribution of the errors presented earlier as well as

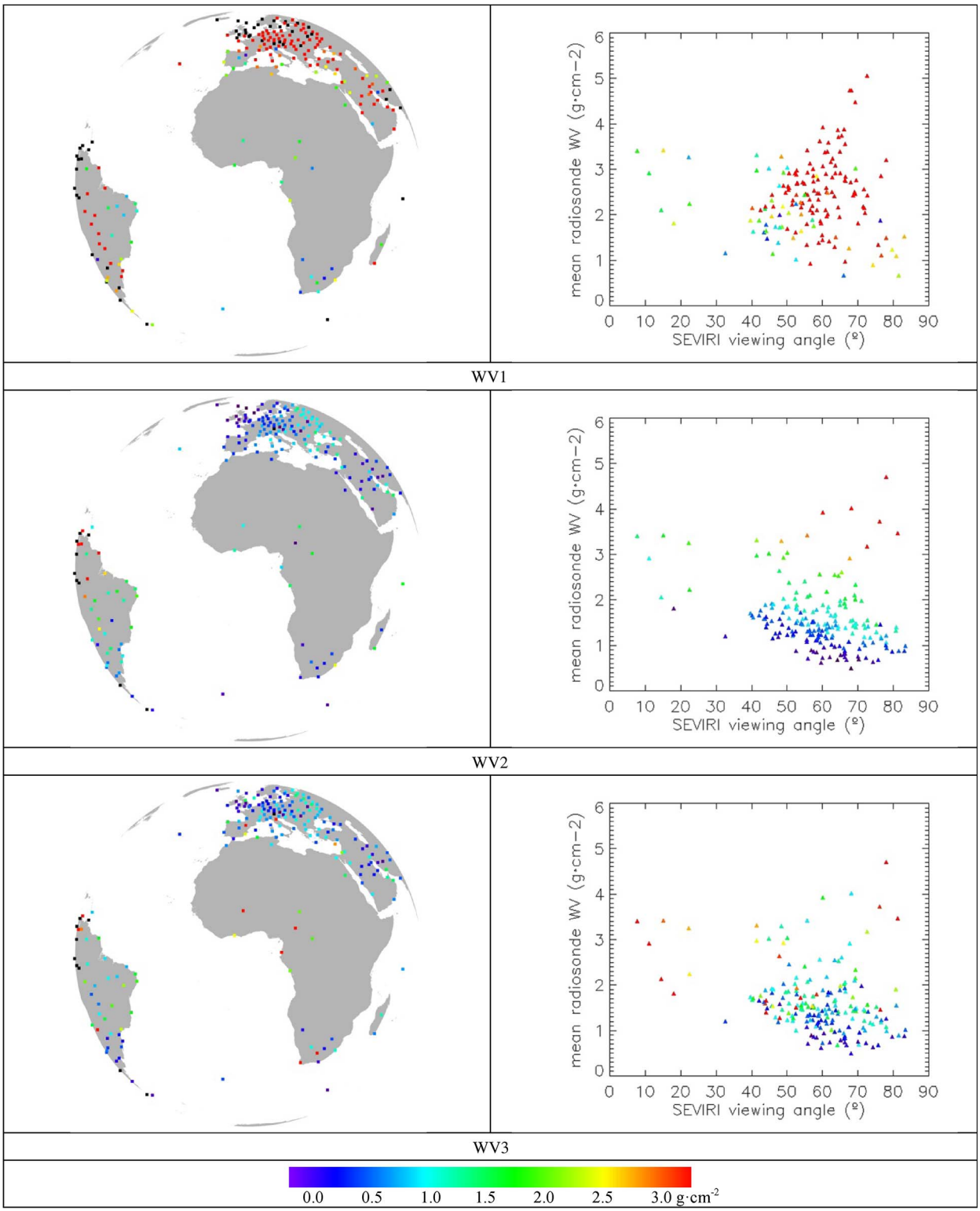

Fig. 2. (Left) RMSE between WV column from radiosonde stations and WV column from MSG-SEVIRI data estimated through (1)–(3) for all available data in 2010. (Right) Scatter plots of RMSE (colorbar) as a function of both SEVIRI viewing angle (horizontal axis, in degrees) and mean radiosonde WV (vertical axis, in grams per square centimeter) for (1)–(3). Black indicates stations for which no valid radiosonde and/or MSG-SEVIRI data are available.

their dependence on both SEVIRI viewing angle and mean radiosonde WV for each of the WV algorithms (see Fig. 2), one can observe that the errors for WV1 have a clear angular dependence, with WV1 estimates unavailable for the outer portion of MSG-SEVIRI disk, due to the high amount of data needed by the algorithm, and high errors (above 3 $\mathrm{g \cdot cm^{-2}}$) decreasing to lower errors when getting closer to nadir. In that case, including an angular dependence of WV1 coefficients decreased the RMSE of the algorithm (not shown), although not below the RMSE obtained for the other two algorithms.

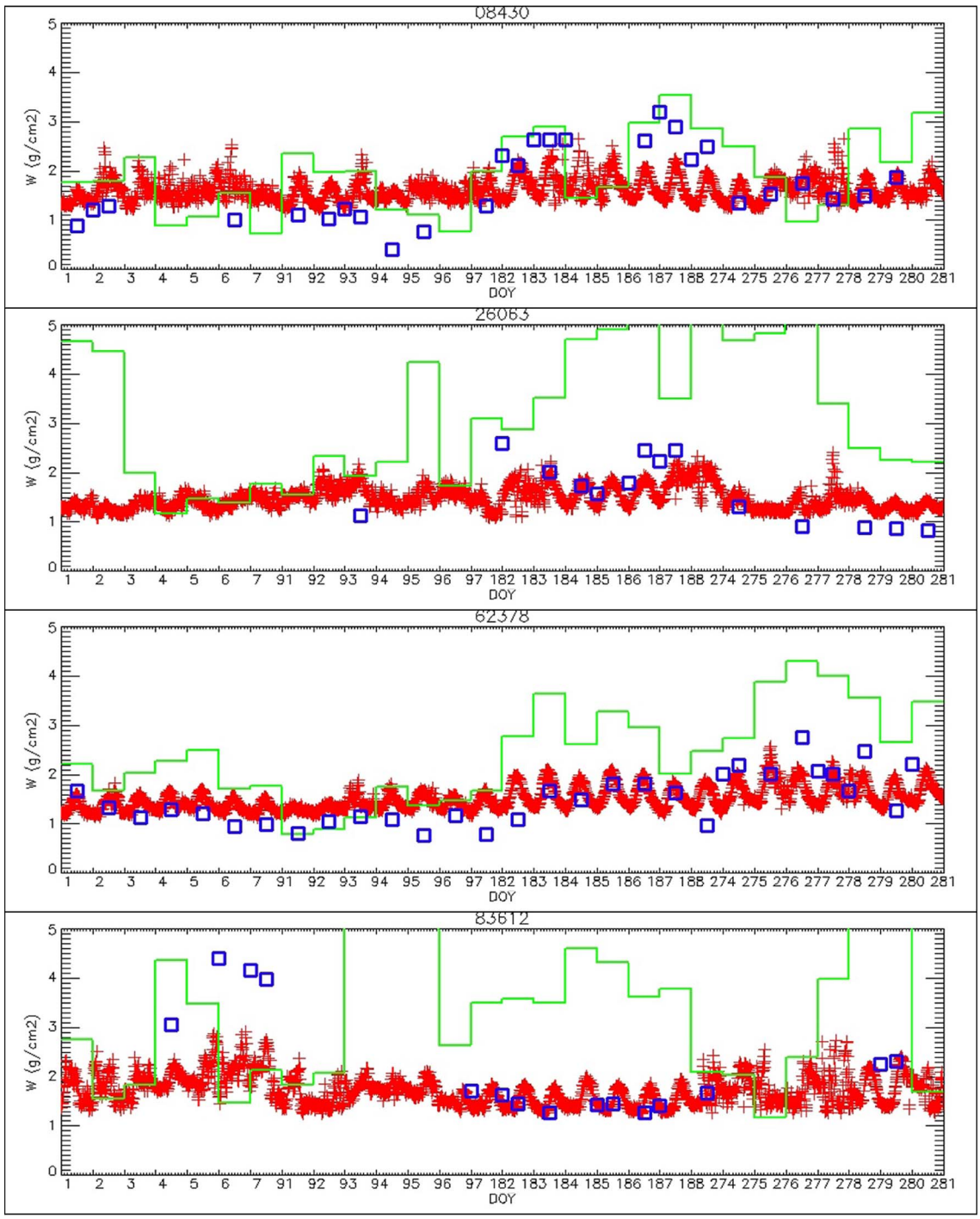

Fig. 3. Time series of WV column retrieved from radiosonde database (blue squares), daily averaged Sobrino and Romaguera [23] algorithm (green line), and (2) (red crosses), at selected radiosonde stations (see Table II), for the first weeks of January, April, July, and October, in 2010.

The WV2 algorithm shows higher errors close to the Equator, particularly when both mean radiosonde WV and SEVIRI viewing angle are high, corresponding to areas where the cloud cover is more frequent and has probably been underestimated by the simple cloud mask we used in this study. For example, most values in Amazonia correspond to the highest observed errors for this algorithm. When we exclude these stations from the RMSE calculation, it drops to 1.04 $g \cdot cm^{-2}$, still twice the lowest errors obtained by other existing algorithms [19], [23]. Finally, the WV3 algorithm shows slightly higher RMSE than the WV2 algorithm, mainly for stations close to SEVIRI nadir. Therefore, we selected the WV2 algorithm to estimate WV instantaneously from MSG-SEVIRI, and hereafter, we analyze more thoroughly the validity of the retrieved WV for this algorithm only.

To have a closer look at the time series of retrieved WV, and in order to compare with existing algorithms, we estimated WV from WV2, on one hand, and from the method developed by Sobrino and Romaguera [23], on the other hand, for the whole MSG-SEVIRI disk for the first week of January, April, July, and October, in 2010. Sobrino and Romaguera [23] WV estimates (WVSR) were summarized as daily averages, by estimating

TABLE II
CHARACTERISTICS OF RADIOSONDE STATIONS USED FOR METHOD VALIDATION AND COMPARISON (SEE FIG. 3)

ID	Name	Coordinates
08430	Murcia, Spain	38.00, -1.16
26063	Voyeykovo, Russia	59.95, 30.70
62378	Helwan, Egypt	29.860N; 31.330E
83612	Campo Grande, Brazil	-20.46, -54.66

WV for any possible 6-h time lapse within a given day, considering as valid only the pixels for which the temperature during these 6-h time lapses had experienced a change above 10 K. This allows a reduction of WVSR daily dispersion (not shown) associated to the uncertainty regarding the "effective hour" to which each 6-h time lapse should be affected. Fig. 3 presents the resulting WV time series at four selected radiosonde stations, using SEVIRI WV estimates closest in space to their geographical location. These stations were selected as belonging to different countries and/or atmospheric conditions among the 53 stations, which had an average of at least one clear-sky observation every two days. Their names and geographical coordinates are indicated in Table II. Compared to radiosonde data, WV2 estimates are generally in agreement, although some slight discrepancies can be observed for low (station 08430, DOY 94–95) and high values (station 08430, DOY 186–188; station 26063, DOY 182; station 83612, DOY 4–7). On the other hand, WVSR estimates tend to diverge from radiosonde data, except for station 08430 where the overall agreement is comparable to the one reached with WV2. This finding is surprising since WVSR estimates are expected to have a better accuracy than WV2, although more investigation is needed to draw definitive conclusions. One can observe higher values for radiosonde stations, which may correspond to undetected cloud presence, as could be inferred from the vertical dispersion for simultaneous observations in SEVIRI WV2. This is clearly the case for the first four observations of the bottom graph in Fig. 3 (Campo Grande, Brazil). Finally, for all four stations, the WV2 algorithm shows a clear diurnal pattern, with seasonal variations in amplitude, although WV2 daily minimum tends to remain stable through the year.

However, these discrepancies do not lead to high differences in resulting LST. Fig. 4 shows the root-mean-square difference (RMSD) between retrieved LST using Atitar and Sobrino [4] algorithm with WV estimated from WV2 and WVSR equations, all other parameters (emissivities) being equal, for the same period as earlier. In this figure, we can see that the resulting difference in LST is low for most viewing angles (below 0.5 K), except for the highest viewing angles ($> 70^\circ$) where the optical path through the atmosphere is increased, and LST estimation errors increase substantially.

Additionally, we performed a sensitivity analysis of the SW LST retrieval algorithms, as presented in Jiménez-Muñoz and Sobrino [8]. In this way, we can predict errors on LST due to uncertainties in WV content. According to the sensitivity analysis, an uncertainty of 0.5, 1, and 1.5 $\mathrm{g \cdot cm^{-2}}$ in WV estimation leads to errors in LST retrieval of 0.13, 0.23, and 0.39 K, respectively. These error values are low in comparison with other error sources in LST retrieval, particularly the uncertainty on surface emissivity, which leads to an error in LST retrieval around 1 K. Therefore, the high WV error of around

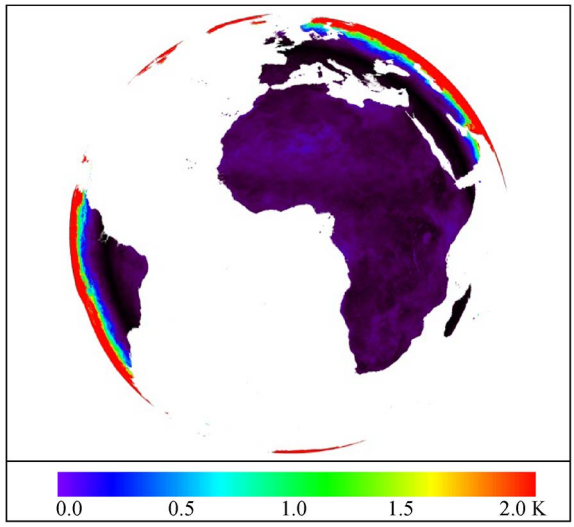

Fig. 4. RMSD between LSTs estimated for the first weeks of January, April, July, and October, in 2010, by using Atitar and Sobrino [4] LST algorithm with WV column estimated with the methods of Romaguera and Sobrino [22] versus (2).

$1\ \mathrm{g \cdot cm^{-2}}$ obtained with WV2 can be still accepted to retrieve LST with SW algorithm.

Validation of the WV2 algorithm shows higher RMSE errors ($1\ \mathrm{g \cdot cm^{-2}}$) than the ones reported for other algorithms in the literature [19], [23]. However, Fig. 4 and error propagation analysis show that the resulting error increase in LST estimation is negligible, to be compared with an increased simplicity in WV estimation. As stated earlier, the two other available methods need a difference of 5 to 10 K between two images to retrieve accurate WV amount. However, in a near-real-time processing chain, these methods are tricky to implement. For instance, one can use a previous image acquired X hours earlier ($X = 6$ in the implementation we used earlier for the Sobrino and Romaguera [23] algorithm). However, nothing guarantees that the temperature difference between these two acquisitions will be enough for the applicability of the chosen method, since this temperature difference depends directly on the temperature daily cycle of the considered pixel location. Not to mention the fact that the implicit assumption of these methods is that WV remains constant during these X hours, in contradiction to time series of WV2 estimates in Fig. 3. The simplicity of the proposed approach allows a straightforward estimation of WV, which makes this approach well suited for the instantaneous retrieval of MSG-SEVIRI LST. On the other hand, we do not recommend this method for strict WV estimation, since already existing methods [19], [23] have been shown to provide WV estimates with better accuracy, although their formulation prevents their use in any near-real-time MSG-SEVIRI processing, in opposition with the method (WV2) presented here.

V. CONCLUSION

This paper has investigated three algorithms to retrieve instantaneously the total amount of WV from MSG-SEVIRI data. Among these three algorithms, one (WV2), based on only three MSG-SEVIRI bands, has been shown to produce smaller errors, although these errors are twice the errors reported in previous works. When compared with the algorithm previously used

by the authors to estimate WV, as well as independent data from radiosoundings, the novel algorithm behaves correctly. Moreover, error propagation analysis and direct comparison show that the increased error of this novel WV algorithm can be neglected when estimating LST. Therefore, this straightforward algorithm (WV2) has been implemented in the near-real-time MSG-SEVIRI processing chain of the receiving station located at the Global Change Unit of the University of Valencia, Spain, and could be implemented in other MSG-SEVIRI receiving stations as well.

ACKNOWLEDGMENT

The authors would like to thank the members of the Global Change Unit of the University of Valencia for their dedication in keeping the MSG receiving-station running over the years, and the University of Wyoming for providing free access to their radiosoundings database.

REFERENCES

[1] F. Aires, A. Chédin, N. A. Scott, and W. B. Rossow, "A regularized neural net approach for retrieval of atmospheric and surface temperatures with the IASI instrument," *J. Appl. Meteorol.*, vol. 41, no. 2, pp. 144–159, Feb. 2002.

[2] M. Amraoui, C. C. DaCamara, and J. M. C. Pereira, "Detection and monitoring of African vegetation fires using MSG-SEVIRI imagery," *Remote Sens. Environ.*, vol. 114, no. 5, pp. 1038–1052, May 2010.

[3] M. Atitar and J. A. Sobrino, "A split-window for estimating LST from Meteosat 9 Data: Test and comparison with *in situ* data and MODIS LSTs," *IEEE Geosci. Remote Sens. Lett.*, vol. 6, no. 1, pp. 122–126, Jan. 2009.

[4] A. M. Baldridge, S. J. Hook, C. I. Grove, and G. Rivera, "The ASTER spectral library version 2.0," *Remote Sens. Environ.*, vol. 113, no. 3, pp. 711–715, Apr. 2009.

[5] A. Berk *et al.*, *MODTRAN4 User's Manual*. Bedford, MA, USA: Air Force Research Laboratory, Hanscom AFB, 1999.

[6] Y. S. Bennouna *et al.*, "An automated day-time cloud detection technique applied to MSG-SEVIRI data over Western Europe," *Int. J. Remote Sens.*, vol. 31, no. 23, pp. 6073–6093, Jul. 2010.

[7] R. Fensholt *et al.*, "Analysing the advantages of high temporal resolution geostationary MSG SEVIRI data compared to Polar Operational Environmental Satellite data for land surface monitoring in Africa," *Int. J. Appl. Earth Observ. Geoinf.*, vol. 13, no. 5, pp. 721–729, Oct. 2011.

[8] J. C. Jiménez-Muñoz and J. A. Sobrino, "Split-window coefficients for land surface temperature retrieval from low-resolution thermal infrared sensors," *IEEE Geosci. Remote Sens. Lett.*, vol. 5, no. 4, pp. 806–809, Oct. 2008.

[9] G. Laneve, M. M. Castronuovo, and E. G. Cadau, "Assessment of the fire detection limit using SEVIRI/MSG sensor," in *Proc. IEEE IGARSS*, 2006, pp. 4157–4160.

[10] M. Lazri *et al.*, "Rainfall estimation over a Mediterranean region using a method based on various spectral parameters of SEVIRI-MSG," *Adv. Space Res.*, vol. 52, no. 2, pp. 1450–1466, Oct. 2013.

[11] Z.-L. Li *et al.*, "Satellite-derived land surface temperature: Current status and perspectives," *Remote Sens. Environ.*, vol. 131, pp. 14–37, Apr. 2013.

[12] Z.-L. Li *et al.*, "Land surface emissivity retrieval from satellite data," *Int. J. Remote Sens.*, vol. 34, no. 9/10, pp. 3084–3127, May 2013.

[13] L. Lu, V. Venus, A. Skidmore, T. Wang, and G. Luo, "Estimating land-surface temperature under clouds using MSG/SEVIRI," *Int. J. Appl. Earth Observ. Geoinf.*, vol. 13, no. 2, pp. 265–276, Apr. 2011.

[14] C. Mattar, J. A. Sobrino, Y. Julien, and L. Morales, "Trends in column integrated water vapour over Europe from 1973 to 2003," *Int. J. Climatol.*, vol. 31, no. 12, pp. 1749–1757, 2010.

[15] H. Nieto, I. Aguado, E. Chuvieco, and I. Sandholt, "Dead fuel moisture estimation with MSG-SEVIRI data. Retrieval of meteorological data for the calculation of the equilibrium moisture content," *Agric. Forest Meteorol.*, vol. 150, no. 7/8, pp. 861–870, Jul. 2010.

[16] H. Nieto, I. Sandholt, I. Aguado, E. Chuvieco, and S. Stisen, "Air temperature estimation with MSG-SEVIRI data: Calibration and validation of the TVX algorithm for the Iberian Peninsula," *Remote Sens. Environ.*, vol. 115, no. 1, pp. 107–116, Jan. 2011.

[17] R. Ross and W. P. Elliott, "Tropospheric water vapor climatology and trends over North America: 1973–93" *J. Climate*, vol. 9, no. 12, pp. 3561–3574, Dec. 1996.

[18] A. Ruescas, M. Arbelo, J. A. Sobrino, and C. Mattar, "Examining the effect of the dust aerosol on satellite sea surface temperatures in the Mediterranean sea using the Medspiration match-up database," *J. Atmosp. Ocean. Technol. A*, vol. 28, no. 5, pp. 684–697, May 2011.

[19] M. Schroedter-Homscheidt, A. Drews, and S. Heise, "Total water vapor column retrieval from MSG-SEVIRI split window measurements exploiting the daily cycle of land surface temperatures," *Remote Sens. Environ.*, vol. 112, no. 1, pp. 249–258, Jan. 2008.

[20] J. A. Sobrino, Z.-L. Li, and M. P. Stoll, "Impact of the atmospheric transmittance and total water vapor content in the algorithms for estimating satellite sea surface temperatures," *IEEE Trans. Geosci. Remote Sens.*, vol. 31, no. 5, pp. 946–952, Sep. 1993.

[21] J. A. Sobrino, Y. Julien, and G. Sòria, "Estimation of land surface phenology from Meteosat Second Generation SEVIRI data (2008–2011)," *IEEE J. Sel. Topics Appl. Earth Observ. Remote Sens.*, vol. 6, no. 3, pp. 1653–1659, Jun. 2013.

[22] J. A. Sobrino and M. Romaguera, "Land surface temperature retrieval from MSG-SEVIRI data," *Remote Sens. Environ.*, vol. 92, pp. 247–254, 2004.

[23] J. A. Sobrino and M. Romaguera, "Water vapour retrieval from Meteosat 8/SEVIRI observations," *Int. J. Remote Sens.*, vol. 29, no. 3, pp. 741–754, Feb. 2008.

[24] D. Sun and R. T. Pinker, "Retrieval of surface temperature from the MSG-SEVIRI observations: Part I. Methodology," *Int. J. Remote Sens.*, vol. 28, no. 23, pp. 5255–5272, Dec. 2007.

[25] J. Wang and W. B. Rossow, "Determination of cloud vertical structure from upper-air observations," *J. Appl. Meteorol.*, vol. 34, no. 10, pp. 2243–2258, Oct. 1995.

Yves Julien received the Ph.D. degree in earth physics and thermodynamics from the University of Valencia, Valencia, Spain, in 2008 and the Ph.D. degree in electronics, electrotechnics, and automatics (specialized in remote sensing) from the University of Strasbourg, Strasbourg, France.

He is a Researcher with the Global Change Unit, University of Valencia. He is the author of more than 30 international papers. His research interests include temperature and vegetation index interactions as well as time series analysis for land cover dynamic monitoring.

José A. Sobrino is a Professor of physics and remote sensing, the President of the Spanish Association of Remote Sensing, and the Head of the Global Change Unit at the University of Valencia, Valencia, Spain. He is the author of more than 150 papers and the Coordinator of the European projects WATERMED and EAGLE. His research interests include atmospheric correction in visible and infrared domains, the retrieval of emissivity and surface temperature from satellite images, and the development of remote sensing methods for land cover dynamic monitoring.

Dr. Sobrino has been a member of the Earth Science Advisory Committee of the European Space Agency since November of 2003. He is the Chairperson of the series of International Symposiums on Recent Advances in Quantitative Remote Sensing.

Cristian Mattar received the Ph.D. degree in physics from the University of Valencia, Valencia, Spain, in 2011.

He is currently a Research Scientist with the Laboratory for Analysis of the Biosphere, Department of Environmental Sciences, University of Chile, Santiago, Chile. His main research interests include calibration and validation of remote sensing products, soil moisture estimates, and long-term trend analysis.

Juan C. Jiménez-Muñoz received the Ph.D. degree in physics from the University of Valencia, Valencia, Spain, in 2005.

He is currently a Research Scientist in the Global Change Unit of the Image Processing Laboratory at the University of Valencia, where he has been an Assistant Professor in the Department of Earth Physics and Thermodynamics, Faculty of Physics, since 2010. His main research interests include applications of thermal remote sensing and land surface temperature and emissivity retrieval.